Algal Research 78 (2024) 103393

Contents lists available at ScienceDirect

Algal Research

journal homepage: www.elsevier.com/locate/algal

Unveiling the anti-proliferative and pro-thermogenic activity of *Staurosirella pinnata* (Bacillariophyta) bioproducts

Saverio Savio [a,b,*], Riccardo Turchi [a], Marianna Carbone [c,*], Maria Letizia Ciavatta [c], Daniele Lettieri-Barbato [a], Katia Aquilano [a], Carlo Rodolfo [a,1], Roberta Congestri [a,1]

[a] Department of Biology, University of Rome Tor Vergata, Rome, Italy
[b] PhD Program in Evolutionary Biology and Ecology, University of Rome Tor Vergata, Rome, Italy
[c] Institute of Biomolecular Chemistry (ICB) of National Research Council (CNR), Pozzuoli, Italy

ARTICLE INFO

Keywords:
Bioactive compounds
Apocarotenoids
Microalgae biotechnology
Biorefinery
Cancer research

ABSTRACT

Biorefinery co-products obtained from biomass of the field isolated diatom *Staurosirella pinnata* have been investigated for their bioactivity on selected human and murine cell lines. Biomass grown in indoor photobioreactor, collected at the stationary phase, was subjected to methanolic extraction to produce a crude extract, sequentially fractionated (hydrophilic-hydrophobic gradient) to obtain six fractions (A4, A5, A7; B4, B5, B6). Fractions' bioactivity was tested on $BRAF^{wt}$ and $BRAF^{V600E}$ human melanoma cell lines, compared to normal keratinocytes. All fractions showed cytotoxic activity, but only fraction A4 showed a remarkable cell-type selectivity, with cell death induction up to 70 % on melanoma cells. Further characterization allowed to identify and purify four apocarotenoids from fraction A4, representing the first report of such class of compound s in mass cultivated diatoms. In addition, fraction A5 resulted to be a mixture of oxylipins and fraction B4 of purine nucleosides, with adenosine as main component. Residual biomass was further processed to obtain an enriched lipidic extract, characterized by a high content of poly-unsaturated fatty acids. Anti-diabetic and anti-obesity activities were assessed by evaluating the expression levels of key proteins involved into thermogenesis (UCP1), lipolysis (Perilipin, HSL660), and mitochondrial dynamics (pDRP1, VDAC), on murine white adipocyte cell line. Overall, the data here reported confirmed *S. pinnata* as a platform for the discovery and purification of bioactive compounds with biomedical potential, and the biorefinery pipeline allow their combined isolation, thus advancing the sustainability of diatom exploitation for the discovery and production of bioactive molecules.

1. Introduction

Microalgae, aquatic photosynthetic microorganisms, are considered an untapped source of bioproducts to exploit in a range of biotechnological fields, meeting the current demand for blue technologies and transition to a greener and circular economy. Indeed, thanks to their 'microbe' growth rates and the ease of growth in culture, microalgae are currently explored in agriculture, as fertilizers and biopesticides, in feed production, wastewater treatment, bioenergy, and human health and nutrition. Also, thanks to their 'tuneable' cell biochemistry, under defined stress conditions applied in closed growth systems or photobioreactors, microalgae proved promising for the discovery of novel bioactive molecules and their development as drugs (*e.g.*, drug discovery). Indeed, reports on microalgal extract bioactivities on human cells are rapidly increasing, highlighting immunomodulatory [1], neuro- [2] and cardio-protective effects [3] as well as anti-proliferative and pro-apoptotic activities against cancer cells [4]. In this context, diatoms play a key role. Diatoms are nearly ubiquitous and adaptable microorganisms, able to dominate natural communities thanks to their rapid growth rates and the ability to 'sense' and acquire nutrients (scavenging capacity) from the environment, thus outcompeting other microalgae [5,6]. Also, they produce finely perforated silica cell walls that protect cells from grazers, by conferring strong mechanical resistance [7], from pathogens (viruses and bacteria), through a hydrodynamical defense mechanism [8], and from harmful light radiations [9,10].

Chemical ecology studies revealed that diatom success also relies on

* Corresponding authors.
E-mail addresses: saverio.savio@gmail.com (S. Savio), mcarbone@icb.cnr.it (M. Carbone), lciavatta@icb.cnr.it (M.L. Ciavatta), katia.aquilano@uniroma2.it (K. Aquilano), carlo.rodolfo@uniroma2.it (C. Rodolfo), roberta.congestri@uniroma2.it (R. Congestri).
[1] These authors have contributed equally to this work.

https://doi.org/10.1016/j.algal.2024.103393
Received 31 October 2022; Received in revised form 29 November 2023; Accepted 8 January 2024
Available online 12 January 2024

their ability to produce, in response to environmental triggers, a wide range of secondary metabolites with different bioactive effects. For instance: domoic acid, a well-known unusual amino acid with neurotoxic effects on humans and sea fauna, also able to regulate bacteria in the phycosphere [11–13]; oxylipins, oxygenated fatty acids produced as anti-grazing compounds against sea urchins and copepods [14–17]; sex pheromones; diketopiperazines [18–21]. In recent years, this evidence led to a growing interest towards the biomedical potential of diatoms. Indeed, the unique metabolic capabilities of these organisms, coupled with their diverse biochemical and ecological characteristics, make them a promising source of bioactive compounds. Several studies deal with bioactivity of diatom extracts, especially fucoxanthin enriched products, highlighting their anti-inflammatory [22] and anti-proliferative effects, on a set of human cellular targets [23], as well as their anti-hypertensive [24], anti-microbic [25], and pro-apoptotic [26] properties.

Nevertheless, studies aimed at identifying the bioactive components of diatom extracts are still scanty. [27]. The field could greatly benefit from the application of more rigorous approaches in the screening phase, more exhaustive analysis of the bioactive mechanisms of action, and the application of biorefinery approaches. In the latter, a single biomass is subjected to multiple sequential extraction steps, thus allowing to maximize yield and diversity of extractable compounds, and to increase chances to discover novel, bioactive molecules. Moreover, microalgae biorefinery offers a more profitable process for biomass exploitation, through the use and valorisation of co-products and intermediates, that can be delivered to different biotechnological application.

To date, a limited number of biorefinery protocols have been developed and implemented to explore the potential of microalgae biomass in discovering natural products with biomedical applications. Indeed, this methodology has primarily been focused on biodiesel, fucoxanthin, and protein production in diatoms, such as *Halamphora* sp. [28] and *Phaeodactylum tricornutum* [29], and has been applied to extract lipids, carotenoids, glycerol, and phytosterols from the green microalgae *Dunaliella salina* and *D. tertiolecta* [30,31].

In a previous work, a cascade extraction protocol was developed to explore the biomedical potential of the mass cultivated diatom *Staurosirella pinnata* (Ehrenberg) D.M. Williams & Round [32]. The results showed that molecules isolated from a first hydroalcoholic extraction exhibited strong and selective cytotoxic effect against human melanoma cancer cells, with no adverse effect on non-malignant cells. In addition, further extraction of the residual biomass resulted in the isolation of a Poly-Unsaturated Fatty Acids (PUFAs) rich lipidic extract, with promising potential as nutraceuticals.

Based on these initial findings, the same biorefinery protocol was applied in this work, in order to: i) better define the anti-cancer activity of the crude extract of *S. pinnata*, by implementing the fractionation protocol and testing fractions on melanoma cell lines; ii) characterize the compounds present in bioactive fractions, by NMR and HPLC methods iii) assess the anti-diabetic and anti-obesity potential of the lipidic extract on white adipose tissue cells, by analysing its pro-thermogenic and pro-lipolysis activity.

2. Materials and methods

2.1. Staurosirella pinnata culture

Stock culture of the field isolated strain VRUC 290 (Tor Vergata Rome University Collection) of the diatom species *Staurosirella pinnata* (Ehrenberg) D.M. Williams & Round was maintained in Diatom Medium (DM) and was used as inoculum for the mass cultivation in indoor 8 L photobioreactor at 25 °C and irradiance of 80 μmol photons m^{-2} s^{-1}, with a 12:12 h light/dark cycle, as previously described [32]. To improve biomass production, the culture was pneumatically stirred, and biomass accumulation was monitored every 48 h by measuring both the optical density (OD) at 665 nm and 730 nm, with an Onda UV-30 Scan spectrophotometer. To evaluate the possible presence of contaminants, culture samples were analyzed by light microscopy (Zeiss Axioskop, 40×), over the whole growth. The biomass was harvested at the stationary phase, by settling and centrifugation (2.200 x*g*, 10 min), freeze-dried (Labcon Lyophilizator), and stored at −80 °C.

2.2. Staurosirella pinnata biorefinery

S. pinnata biomass was sequentially extracted following a cascade extraction protocol developed *ad hoc* [32,33] and summarized in Fig. 1. Briefly, the biomass was firstly treated with a solution of CH_3OH (20 % v/v in H_2O) in order to obtain a crude extract, which was subquently fractionated; then, the residual biomass was treated with $CHCl_3$ and CH_3OH to obtain a lipidic extract. The crude extract fractions and the lipidic extract were then tested on human and murine cell lines, melanoma cancer cells and white adipose tissue cells, in order to evaluate their bioactivity.

2.2.1. Crude extract

Crude extract was obtained from 30 g of lyophilized biomass; the biomass was resuspended in 600 mL of ultrapure water and CH_3OH (20 % v/v), sonicated at 500 W (Q700CA Sonicator) for 2 min and incubated for 2 h at 45 °C, in a thermostatic water bath. Then, the solution was centrifuged (3.200 ×*g*, 20 min), the supernatant collected and vacuum concentrated (Buchi Rotavapor WaterBath B-480), till the evaporation of the organic solvent.

2.2.2. Lipidic extract

The lipidic extract was obtained from the residual biomass, resulting from the methanolic extraction, following the protocol of Bligh and Dyer [34]. Briefly, the residual biomass was grinded for 10 min, suspended in $CHCl_3$:CH_3OH (2:1 v/v), and then centrifuged (2.200 ×*g*, 3 min). The supernatant was collected, the pellet repeatedly washed with $CHCl_3$:CH_3OH (2:1 v/v), and centrifuged (2.200 ×*g*, 3 min), till it turned whitish. The collected supernatants were pooled and treated with 0.1 M HCl/0.5 % $MgCl_2$ and then centrifuged (2.200 ×*g*, 3 min) to separate proteins from lipids. The lower phase, containing lipids, was recovered, vacuum evaporated, and finally the lipidic extract was lyophilized.

2.3. Chemical analysis

2.3.1. General procedures

Solvents were purchased from VWR International. Solid phase extraction (SPE) was performed on Macherey-Nagel C18 Chromabond cartridges. Silica-gel chromatography was realized on precoated Merck F254 plates (TLC). The spots on TLC were visualized under UV light (254 nm) and then sprayed with 10 % H_2SO_4 in water, followed by heating. HPLC purification was carried out on a Jasco system (PU4180 pump equipped with a Jasco UV/Vis detector PU4075) using a semi-preparative column (C18 Ascentis, Supelco, 250 × 10 mm). ESIMS were acquired on a Micromass Q-TOF MicroTM coupled with an HPLC Waters Alliance 2695. The instrument was calibrated by using a PEG mixture from 200 to 1000 MW (resolution specification 5000 FWHM, deviation <5 ppm RMS in the presence of a known lock mass). High-resolution mass spectra (HRESIMS) were acquired on a Q-Exactive hybrid quadrupole-orbitrap mass spectrometer (Thermo Scientific, San Jose, CA, USA). NMR experiments were recorded at the ICB-NMR Service Centre. Chemical shifts values are reported in ppm and referenced to internal signals of residual protons (CD_3OD, δ_H 3.34, δ_C 49.0 ppm, and $CDCl_3$ δ_H 7.26, δ_C 77.0 ppm). 1D and 2D NMR spectra were acquired on a Bruker Avance-400 spectrometer using an inverse probe fitted with a gradient along the *Z*-axis, on a Bruker Avance III HD 400 MHz spectrometer equipped with a CryoProbe Prodigy, and on a DRX 600 spectrometer (600 MHz for ^{1}H, 150 MHz for ^{13}C) equipped with a three-channel inverse (TCI) CryoProbe.

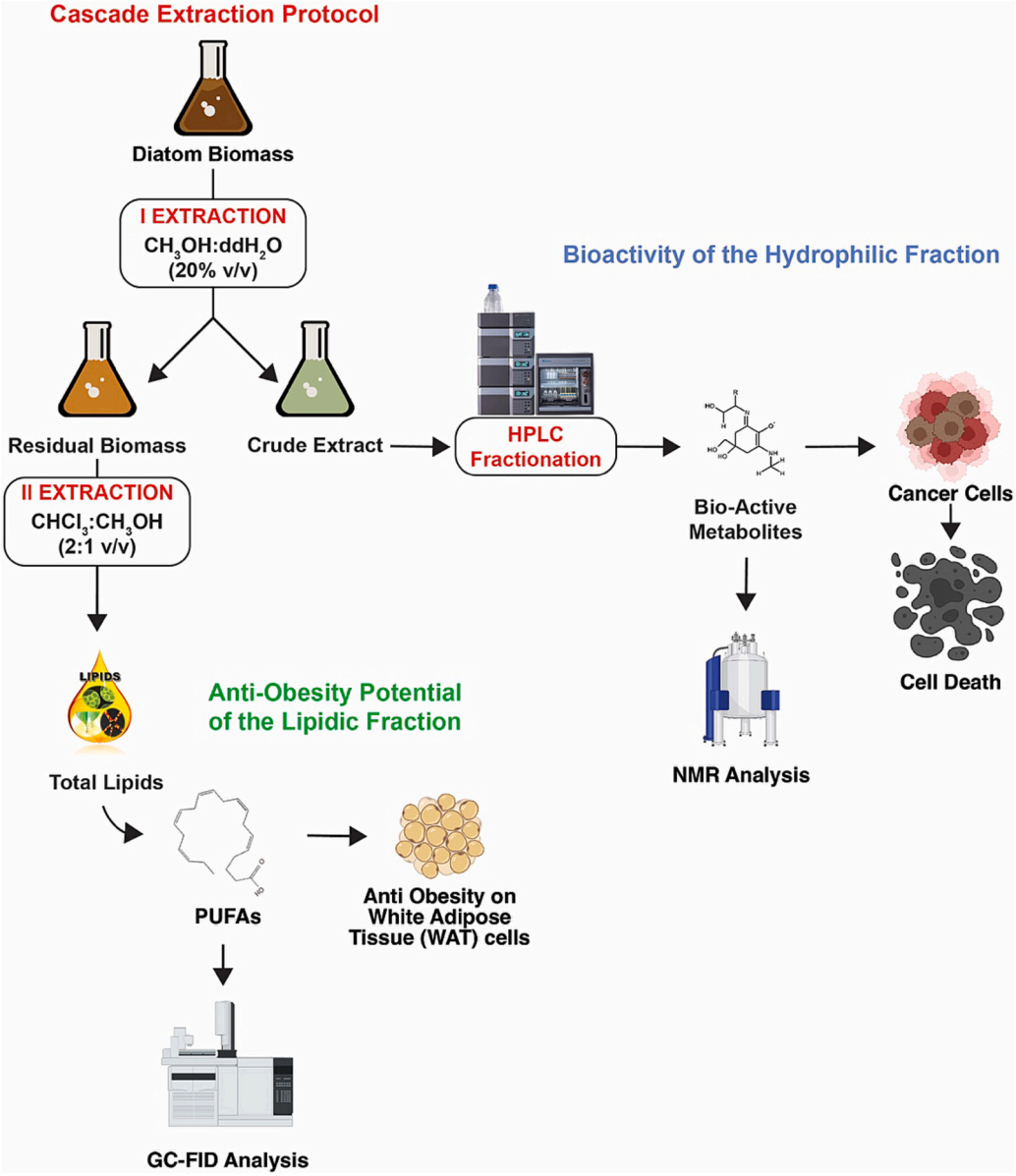

Fig. 1. Scheme of the biorefinery protocol developed in this work.

2.3.2. Fractionation of the crude extract and identification of the main metabolites in selected active fractions

The hydroalcoholic crude extract was subjected to liquid-liquid extraction by partitioning between diethyl ether (EE) and water, and by repartitioning the water layer with *n*-butanol (*n*-BuOH) as to separate the extract in diethyl ether (EE, 293 mg), butanol (BE, 70.8 mg), and aqueous (WE, 356.6 mg) fractions. Then, the EE fraction (280 mg) was subjected to Solid Phase Extraction (SPE) by loading on two C18 cartridge (M-N Chromabond C18 45 mL/5000 mg) each eluted with 20 mL H_2O (fraction A1, 8.7 mg), 50 mL H_2O (fraction A2, 12.4 mg), 40 mL H_2O/MeOH 8:2 (fraction A3, 7.7 mg), 40 mL H_2O/MeOH 1:1 (fraction A4, 14.5 mg), 40 mL H_2O/MeOH 2:8 (fraction A5, 68.6 mg), 40 mL H_2O/MeOH 2:8 (fraction A6, 46.9 mg), and 60 mL MeOH (fraction A7, 130.7 mg). Fractions A1-A7 were preliminary analyzed by ^{1}H NMR.

Fraction A4 was further purified by HPLC on a semipreparative C18 column using a non linear gradient of H_2O/acetonitrile starting from 30 % of acetonitrile to 50 % in 20 min, and then from 50 % to 75% in 10 min. Peaks eluted at Rt 13.6, 19.0, and 23.5 min have been collected and analyzed by 1D and 2D NMR spectroscopy.

Analogously, fraction A5 was subjected to HPLC purification by using a semipreparative C18 column eluted with a linear gradient starting from 70 % of acetonitrile in water to 100 % of acetonitrile in 20 min. The peak eluted at 16.2 min was analyzed using ESI MS-MS fragmentation analysis.

The butanol soluble portion of crude extract, fraction BE (60 mg), was also subjected to SPE carried out on a C18 cartridge (M-N Chromabond C18 hydra 6 mL/500 mg) eluted with 8 mL H_2O (fraction B1, 46.1 mg), 8 mL H_2O (fraction B2, 2.3 mg), 8 mL H_2O (fraction B3, 1.7 mg), 8 mL H_2O/MeOH 8:2 (fraction B4, 7.9 mg), 15 mL H_2O/MeOH 1:1 (fraction B5, 7.8 mg), 15 mL H_2O/MeOH 2:8 (fraction B6, 4.2 mg), 15 mL MeOH (fraction B7, 3.5 mg). Fractions B1-B7 were preliminary analyzed by ^{1}H NMR.

2.3.3. Characterization of the fatty acid content of the lipidic extract

For the qualitative characterization of fatty acids in the lipidic extract, 100 mg of freeze-dried lipids were derivatized and analyzed by Gas Chromatography equipped with a Flame Ionization Detector (GC-FID).

Fatty Acid Methyl Esters (FAMEs) were obtained by trans-esterification using a CH_3OH:H_2SO_4 solution (15:1 v/v), at 60 °C, for 6

h. FAMEs were identified by comparing the retention times of the peaks recorded in the sample with those of an analytical commercial standard of 37 FAMEs, purchased from Supelco (Sigma-Aldrich, Merck group, Germany). FAMEs characterization was carried out using an Agilent 7890 A (Agilent Technologies, California, USA) GC-FID instrument, equipped with a DB-Wax column (30 m × 0.25 mm, i.d. 0.25 μm). Helium (99.999 purity, Abello Linde S.A, Barcellona, Spain) was used as carrier gas (1 mL/min) following the temperature program here reported: column was held at 50 °C for 1 min, ramped to 200 °C, at 25 °C/min, increased to 230 °C, at 3 °C/min, and then held for 18 min. FID detector temperature was fixed at 280 °C. Data were compared to those reported in Savio et al. 2020 [32] to evaluate the stability and reproducibility of FAME composition in the lipidic extracts through different mass cultivation run.

2.4. Bioactivity test on human and murine cell lines of the crude extract fractions and of the lipidic extract

2.4.1. Bioactivity assay of crude extract fractions on melanoma cancer cells

CHL-1 ($BRAF^{wt}$) and A375 ($BRAF^{V600E}$) human melanoma and human immortalized keratinocytes (HaCaT) cell lines (American Type Culture Collection, ATCC, USA), were cultured in high-glucose Dulbecco Modified Eagle Medium (DMEM), supplemented with 10 % heat-inactivated foetal bovine serum (FBS), penicillin (100 U/mL), and streptomycin (100 μg/mL), at 37 °C in a 5 % CO_2 humidified atmosphere. For the bioactivity assays cells were seeded in 12-well plates (5×10^4 cells/well) and the next day treated with *S. pinnata* crude extract's fractions (100 mg/mL in DMEM), at the concentrations of 0.125, 0.250, and 0.500 mg/mL, for 24 h. At the end of the treatment, cells were detached with trypsin, washed twice in PBS, and suspended in propidium iodide solution. Cell death and cell cycle analyses were performed by means of flow cytometry, as previously described [35].

2.4.2. Bioactivity assay of the lipidic extract on white adipose tissue cells

3T3-L1 murine preadipocytes (ATCC, USA) were cultured in DMEM medium supplemented with 10 % Newborn Serum, 1 % non-essential amino acids (NEAA), penicillin (100 U/mL) and streptomycin (100 μg/mL), and 2 mM glutamine (Lonza Sales, Basel, Switzerland). 3T3-L1 differentiation into adipocytes was achieved by adding differentiation medium (DMEM, 10 % of foetal bovine serum, 0.5 mm 3-isobutyl-1-methylxanthine, 1 μM dexamethasone, and 1.7 μM insulin) every 48 h, as previously reported [36]. After 8 days of differentiation, the differentiation medium was replaced with maintenance medium (DMEM) and cells were used for the experiments.

For the bioactivity assays, the lipidic extract of *S. pinnata* was conjugated with Bovine Serum Albumin (BSA). Briefly, 50 mM of the lipidic extract was dissolved in 2 mL of a solution of NaOH 0.1 M, stirred at 70 °C until the dissolution of lipids in the solution was occurred, and incubated at 37 °C with 0.6 mL of ddH_2O and BSA (10 %). Then, conjugated lipids were administered on 3T3-L1 cells for 24 h, at concentrations of 30 and 60 μg/mL. After the treatments, cells were collected and stored at −20 °C for Western Blotting analyses.

2.4.3. Gel electrophoresis and Western blotting

Cells were lysed in RIPA buffer (50 mM Tris-HCL pH 8.0, 150 mM NaCl, 0.1 % SDS, 0.5 % sodium deoxycholate, 1 % NP-40) supplemented with protease inhibitors cocktail (VWR life sciences). Western blotting analysis was performed by using the following antibodies: anti-HSL (4107, Cell Signalling Technology), anti-p-HSL660 (4126 T, Cell Signalling Technology), anti-VDAC1 (sc-8828, Santa Cruz Biotechnology), anti-UCP1 (CS-14670S, Cell Signalling Technology), anti-DRP1 (6,111,738, BD Transduction Laboratories™, San Jose, CA, USA), anti-p-DRP1 (ser637) (4867, Cell Signalling Technology) Anti-PLIN-1 (3470 Cell Signalling Technology).

2.5. Data analysis

GraphPad Prism version 9.0 program (GraphPad Software, San Diego, CA, USA) was used for statistical analysis. Two-Way ANOVA and Tukey's HSD test were performed (a p-value of <0.05 was considered statistically significant) and standard deviations (SD) were calculated and reported.

3. Results and discussion

3.1. Bioactivity of crude extract fractions on A375 and CHL-1 melanoma cancer cells

The bioactive potential of the different fractions, obtained from the first hydroalcoholic extraction, was evaluated by assessing their ability to induce cell death in a 24 h dose-response assay. To this aim, we compared two different human melanoma cell lines, CHL-1 ($BRAF^{wt}$) and A375 ($BRAF^{V600E}$), to normal human keratinocyte (HaCaT) (Fig. 2).

All tested fractions showed a cytotoxic effect, although some differences were observed depending on both fractions and cell lines. In fact, the administration of fraction B4 resulted in a low cell death induction, even at the highest dose (0.500 mg/mL), with no significant differences between melanoma and keratinocyte cell lines. Similarly, the administration of fractions B5 and A5 did not induce significant cell death levels at the lowest dose used (0.125 mg/mL) in both melanoma and keratinocytes, while significant increases of cell death levels were observed at the highest dose. However, also for these fractions, a significant difference between the three cell lines was not observed. On the other hand, fractions B6 and A6 proved to be more effective, with cell death levels up to 60 %, in all the cell lines at the highest dose used. Fraction A4 exhibited the most promising bioactivity at the highest concentration evaluated, showing a significant increase of cell death in the A375 ($BRAF^{V600E}$) human melanoma cell line, as compared to both CHL-1 ($BRAF^{wt}$) and HaCaT cell lines (Fig. 2). These results suggested the existence of some kind of selectivity for melanoma cell lines, especially for the A375, which are normally more resistant to chemotherapeutic agents, with quite limited adverse effects on normal keratinocytes.

To identify unrelated and/or unexpected effects on normal keratinocytes, an additional evaluation was performed to assess the effect of fraction A4 on cell cycle. To this aim, cells treated as above, were subjected to flow cytometry analysis of the cell cycle (Fig. 3).

Results evidenced that A4 fraction administration to the A375 cell line did not result in any clear and dose-dependent cell cycle alteration, with no significant variation of the cell percentages in G1, S, and G2/M phases. A similar behaviour was observed also for the HaCaT cell line, with the only significant variation detected in cells administered with the 0.250 mg/mL dose, showing an increase of cell percentages in S phase (from 20.3 % to 49.8 %) coupled to a decrease of cells in the G2/M phase (from 31.5 % to 9.4 %).

Conversely, the CHL-1 cell line showed a completely different behaviour. In fact, the obtained results highlighted: i) a significant dose-dependent decrease in the percentage of cells in the G1 phase (from 68.8 % to 52.3 %) in cells administered with the 0.500 mg/mL dose; ii) a significant increase in the percentage of cells in the S phase (from 3.6 % to 16.8 % and 16.2 %) at 0.125 mg/mL and 0.250 mg/mL doses; iii) a significant decrease of the percentage of cells in the G2/M phase (from 27.5 % to 14.4 %) at 0.125 mg/mL dose, while at 0.250 and 0.500 mg/mL, the percentages increased to 22.8 % and 34.9 %, respectively.

Taken together, these data suggested that fraction A4 could contain promising bioactive compounds, able to induce cell death, but possibly also to impact on DNA integrity, as suggested by the increase of cells in G2/M phase, and/or on the activity of cyclins/CDKs complexes that control cell cycle progression. Moreover, the different behaviour observed between $BRAF^{wt}$ and $BRAF^{V600E}$ melanoma cell lines, suggested that the cytotoxic effect could depend upon the modulation of different signalling pathways. Indeed, as the highest levels of cell death

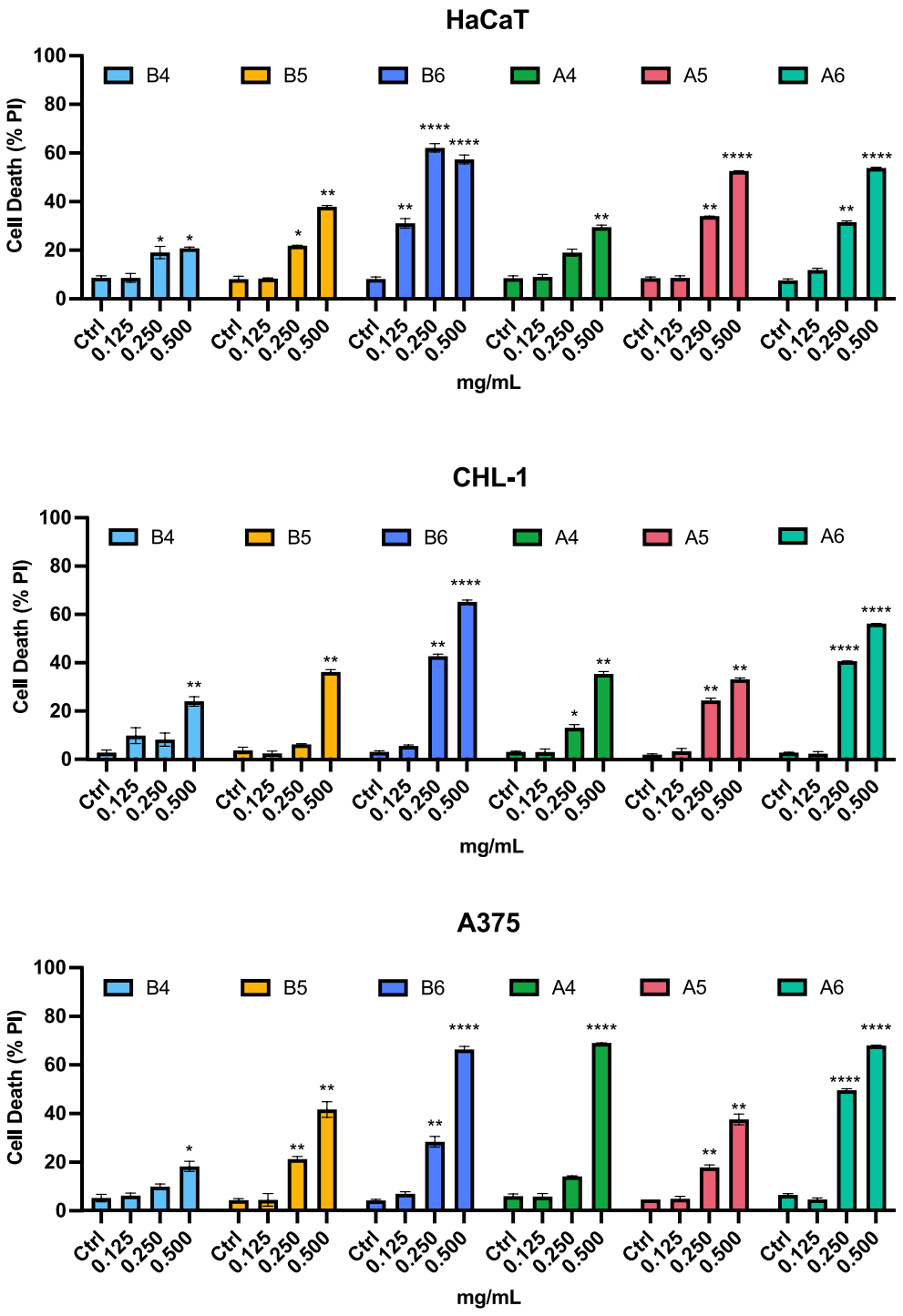

Fig. 2. Cell death induction after administration of crude extract fractions to human melanoma (A375 and CHL-1) and keratinocyte (HaCaT) cell lines. Cell lines were incubated, for 24 h, with the indicated amount of crude extract fractions, and cell death quantified as the percentage of hypodiploid events. *, $p < 0.05$; **, $p < 0.01$; ****, $p < 0.0001$, compared to controls. "Ctrl" refers to cells grown in DMEM.

induction were observed in the A375 cell line, which is characterized by a constitutive activation of the pro-survival MEK/ERK pathway [37], the presence of molecules able to specifically affect this pathway can be hypothesized.

Cell-type selectivity of a bioactive molecule is a critical requirement since the early stages of a bio-screening test [23]. Surprisingly, there is a remarkable scarcity of studies dedicated to investigating the cell-type selectivity using microalgal extracts, despite its utmost importance. Indeed, the potential of microalgae derived metabolites and/or extracts towards cancer cell lines has been already described for mass cultivated commercial strains of the diatom *Skeletonema marinoi* CCMP2092 and the haptophyte *Isochrysis galbana* CCMP1323, showing antiproliferative effects on a number of human cancer cells, including leukaemia (K562), melanoma (A2058), lung cancer (A549), and hepatocarcinoma (HepG2) [38,39], but no chemical characterization of the extracts' composition was provided. On the other hand, amphidinol 22, isolated from the dinoflagellate *Amphidinium carterae*, proved to exert anticancer effects on melanoma cells (A2058), but no tests using no-malignant cells were

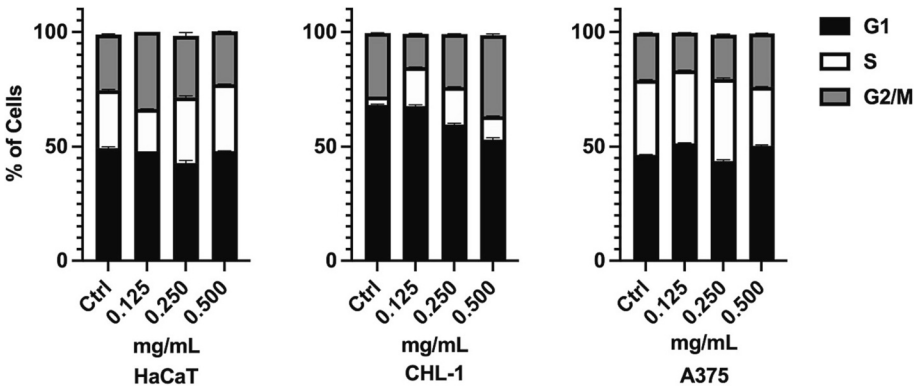

Fig. 3. Cell cycle evaluation after administration of fraction A4 to human melanoma (CHL-1, A375) and keratinocyte (HaCaT) cells lines. Cell lines were incubated, for 24 h, with the indicated amount of fraction A4, and the percentage of cells in the G1, S, and G2/M phases quantified by flow cytometry. "Ctrl" refers to cells grown in DMEM.

performed, preventing any evaluation of amphidinol 22 cell-type selectivity [40].

The observed cell-type selectivity for fraction A4 prompted further investigation into its chemical composition to identify new molecules that could be exploited as anti-cancer drugs.

3.2. Identification of metabolites in selected bioactive crude extract fractions

In order to characterize the bioactive components of fractions A4 and A5, both of them were purified by HPLC methods. The HPLC profile of fraction A4 (Fig. 4) displayed three main peaks, which were subsequently collected and subjected to NMR and MS analysis. The ^{1}H NMR spectrum of P1 peak, eluted at Rt 13.6 min, displayed signals attributable to two compounds with a ratio 60:40. Then, 2D NMR and MS allowed to recognize a nor-isoprenoids skeleton for both compounds and their attribution to two apocarotenoids, the loliolide (**1**) [41] and the 3,5,6-trihydroxy-7-megastigmen-9-one (**2**) [41] by comparison with the literature data. Instead, peaks P2 and P3, eluted at Rt 19.0 min and 23.5 min, resulted to contain other two apocarotenoids identified as Apo-13-fucoxanthinone (**3**) [41] and Apo-9-fucoxanthinone (**4**) [41], respectively by analysis of NMR experiments and MS data (Fig. 5).

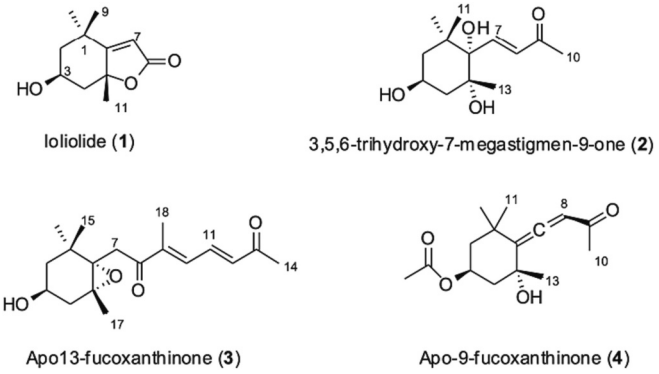

Fig. 5. Main components of fraction A4.

Loliolide (**1**): ^{1}H NMR (CD_3OD, 400 MHz) δ 5.78 (1H, s, H-7), 4.24 (1H, m, H-3), 2.45 (1H, m, H-4a), 2.01 (1H, m, H-2a), 1.80 (3H, s, H_3-11), 1.79 (1H, m, H-4b), 1.58 (1H, m, H-2b), 1.50 (3H, s, H_3-9), 1.30 (3H, s, H_3-10). ^{13}C NMR (CD_3OD, indirect detection from HSQC and HMBC experiments, 400 MHz) δ 185.0 (s, C-6), 175.7 (s, C-8), 112.6 (d,

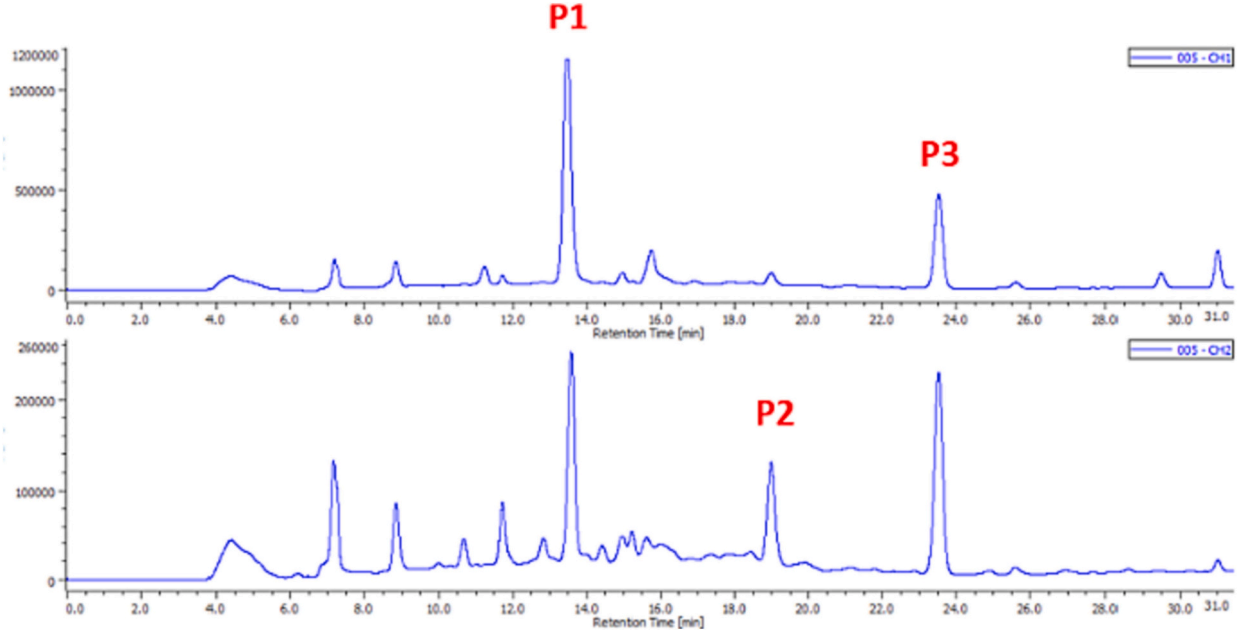

Fig. 4. HPLC profile of fraction A4.

C-7), 89.3 (s, C-5), 66.8 (d, C-3), 47.3 (t, C-2), 46.3 (t, C-4), 36.7 (s, C-1), 30.5 (q, C-10), 27.0 (q, C-11), 26.3 (q, C-9). ESIMS positive mode: *m/z* 219 $[M + Na]^+$.

3,5,6-trihydroxy-7-megastigmen-9-one (**2**): ^{1}H NMR (CD_3OD, 400 MHz) δ 7.20 (1H, d, $J = 15.9$ Hz, H-7), 6.21 (1H, d, $J = 15.9$ Hz, H-8), 3.79 (1H, m, H-3), 2.33 (1H, m, H-4a), 2.32 (3H, s, H_3-10), 1.68 (1H, m, H-4b), 1.62 (1H, m, H-2a), 1.30 (1H, m, H-2b), 1.22 (3H, s, H_3-12), 1.21 (3H, s, H_3-13), 0.99 (3H, s, H_3-11). ^{13}C NMR (CD_3OD, indirect detection from HSQC and HMBC experiments, 400 MHz) δ 201.2 (s, C-9), 145.2 (d, C-7), 133.2 (d, C-8), 70.7 (s, C-6), 69.1 (s, C-5), 64.0 (d, C-3), 47.9 (s, C-1), 39.8 (t, C-4), 35.8 (t, C-2), 30.1 (q, C-12), 26.9 (q, C-10), 24.9 (q, C-11), 19.1 (q, C-13). ESIMS positive mode: *m/z* 265 $[M + Na]^+$.

Apo-13-fucoxanthinone (**3**): ^{1}H NMR (CD_3OD, 400 MHz) δ 7.63 (1H, dd, $J = 15.4$ and 11.0 Hz, H-11), 7.31 (1H, bd, $J = 11.0$ Hz, H-10), 6.59 (1H, d, $J = 15.4$ Hz, H-12), 3.87 (1H, d, $J = 17.0$, H-7a), 3.78 (1H, m, H-3), 2.68 (1H, d, $J = 17.0$, H-7b), 2.39 (3H, s, H_3-14), 2.29 (1H, m, H-4a), 2.06 (3H, s, H_3-18), 171 (1H, dd, $J = 13.5$ and 10 Hz, H-4b) 1.50 (1H, m, H-2a), 1.28 (1H, m, H-2b), 1.22 (3H, s, H_3-17), 1.06 (3H, s, H_3-15), 0.96 (3H, s, H_3-16). Selected ^{13}C NMR (CD_3OD, indirect detection from HSQC and HMBC experiments, 400 MHz) δ 199.7 (s, C-8), 143.6 (s, C-9), 139.4 (d, C-11), 136.9 (d, C-12), 135.4 (d, C-10), 68.1 (s, C-6), 66.4 (s, C-5), 64.1 (d, C-3), 48.0 (t, C-2), 43.0 (t, C-4), 42.8 (t, C-7), 36.2 (s, C-1), 28.8 (q, C-16), 24.2 (q, C-15), 21.0 (q, C-17), 12.4 (q, C-18). ESIMS positive mode: *m/z* 329 $[M + Na]^+$.

Apo-9-fucoxanthinone (**4**): ^{1}H NMR (CD_3OD, 400 MHz) δ 5.89 (1H, s, H-8), 5.41 (1H, m, H-3), 2.27 (1H, m, H-4a), 2.23 (3H, s, H_3-10), 2.06 (3H, s, $\underline{CH_3}CO$), 2.02 (1H, m, H-2a), 1.59 (1H, m, H-4b), 1.49 (1H, m, H-2b), 1.46 (3H, s, H_3-12), 1.42 (3H, s, H_3-13), 1.20 (3H, s, H_3-11). Selected ^{13}C NMR (CD_3OD, indirect detection from HSQC and HMBC experiments, 400 MHz) δ 200.6 (s, C-9), 172.1 (s, $CH_3\underline{CO}$) 119.0 (s, C-6), 100.6 (d, C-8), 71.6 (s, C-5), 68.5 (d, C-3), 46.0 (t, C-2 and C-4), 36.3 (s, C-1), 31.7 (q, C-12), 30.6 (q, C-13), 28.1 (q, C-13), 26.4 (q, C-10), 20.2 (q, $\underline{CH_3}CO$). ESIMS positive mode: m/z 329 $[M + Na]^+$.

Apocarotenoids are a class of molecules derived from both non-enzymatic and enzymatic oxidative cleavage of carotenoids and have been identified in numerous plant species yet. These compounds, that exhibit a high-degree of chemical diversity, act as precursors of phytohormones and are also involed in different crucial processes of plant development, fruit ripening, stress response and defense mechanisms [42,43]. In addition, apocarotenoids serve as signalling molecules, mediating communication and interactions between plants and their rhizosphere, as in mutualistic symbiotic associations like mycorrhizae [44]. In microalgae, the presence of apocarotenoids have been described only in laboratory scale cultures of green microalgae and other few taxa deriving from commercial culture collection (*Chlamydomonas sp.*, *Chlorella sorokiniana, Nannochloropsis gaditana, Tetraselmis chuii*, and *Tisochrysis lutea* [45]). Indeed, only one report deals with apocarotenoid production by diatoms and refers to the model organism *Phaeodactylum tricornutum* that was found to synthesize apofucoxanthinoids that are considered responsible for the toxic effects on the copepod *Tigriopus californicus,* pointing to their feeding deterrence function [46].

From a biotechnological perspective, apocarotenoids are valuable compounds with significant potential in the biomedical field [47]. Within the isolated apocarotenoids from *S. pinnata*, loliolide (**1**), has recently been reported to possess activity against human hepatocarcinoma (HepG2) cells [48], whereas Apo-13- and Apo-9-fucoxanthinone (**3** and **4**) have shown anti-proliferative and pro-apoptotic activities on human colorectal adenocarcinoma (Caco-2) [49]. Additionally, other activities, including anti-inflammatory, anti-neurodegenerative and antioxidant effects, were reported for apocarotenoids extracted from *Crocus sativus* [50].

Despite their biotechnological potential, apocarotenoids are currently underexploited at industrial scale due to their low cellular content in the natural sources found so far (only a few milligrams per kilogram of biomass). Moreover, chemically synthesized apocarotenoids have been reported to have hazardous effects on human health [51]. Therefore, the recovery of apocarotenoids in the diatom *S. pinnata* gives an additional input to investigate the possibility of exploiting these high-productive and environmentally flexible microalgae for a sustainable production of apocarotenoids which relevant human benefits have been increasingly important in the last years. In addition, since these results are related to extracts obtained from biomass collected at the stationary phase of growth, it might be expected that differences and possibly more bioactives content in the other stages of the growth (*e.g.* exponential phase) are present as is foreseen to be explored in the near future.

HPLC purification of fraction A5 resulted in the collection of a main peak at Rt 16.2 min (Fig. 6) that was analyzed by both NMR and mass spectrometry. The NMR data of this fraction were consistent with the presence of two main structurally related oxylipins (1:1 ratio) that were identified as (7*E*)-9-ketohexadec-7-enoic acid (**5**) and (7*E*)-9-hydroxyhexadec-7-enoic acid (**6**) by ESI MS-MS fragmentation analysis (Fig. 7). In particular, the position of double bond at C7-C8 in both compounds was deduced by the diagnostic fragment ion peak observed in collision-induced decomposition spectra at *m/z* 127 $[C_7H_{11}O_2]^-$.

(7*E*)-9-ketohexadec-7-enoic acid (**5**): ^{1}H NMR ($CDCl_3$, 400 MHz) δ 6.82 (1H, m, H-7), 6.09 (1H, d, $J = 15.8$ Hz, H-8), 2.53, app. t, ($J = 7.4$ Hz, H_2-10), 2.35 (2H, m, H_2-2), 2.22 (2H, m H_2-6), 1.65 (2H, m, H_2-3), 1.62 (2H, m, H_2-11), 1.47 (2H, m, H_2-5), 1.38–1.23 (8H, overlapping signals, H_2-4, H_2-12, H_2-13, and H_2-14), 1.31 (2H, m, H_2-15), 0.88 (3H, t, $J = 7.2$ Hz, H_3-16). Selected ^{13}C NMR ($CDCl_3$, indirect detection from HSQC and HMBC experiments, 400 MHz) δ 200.7 (s, C-9), 176.4 (s, C-1), 148.6 (d, C-7), 131.6 (d, C-8), 41.3 (t, C-10), 34.5 (t, C-2), 33.6 (t, C-6), 25.7 (t, C-3), 22.0 (t, C-15), 15.5 (q, C-16). ESIMS positive mode: *m/z* 291 $[M + Na]^+$. ESIMS negative mode: m/z 267 $[M-H]^-$.

(7*E*)-9-hydroxyhexadec-7-enoic acid (**6**): ^{1}H NMR ($CDCl_3$, 400 MHz) δ 5.62 (1H, m, H-7), 5.45 (1H, dd, $J = 15.3$ and 7.2 Hz, H-8), 4.03 (1H, m, H-9), 2.35 (2H, m, H_2-2), 2.02 (2H, m H_2-6), 1.65 (2H, m, H_2-3), 1.50–1.43 (2H, m, H_2-10), 1.36 (2H, m, H_2-5), 1.38–1.23 (8H, overlapping signals, H_2-4, H_2-12, H_2-13, and H_2-14), 1.31 (2H, m, H_2-15), 0.88 (3H, t, $J = 7.2$ Hz, H_3-16). Selected ^{13}C NMR ($CDCl_3$, indirect detection from HSQC and HMBC experiments, 400 MHz) δ 176.4 (s, C-1), 134.3 (d, C-8), 133.4 (d, C-7), 74.8 (d, C-9), 38.0 (t, C-10), 34.5 (t, C-2), 33.6 (t, C-6), 25.7 (t, C-3), 22.0 (t, C-15), 15.5 (q, C-16). ESIMS positive mode: m/z 293 $[M + Na]^+$. ESIMS negative mode: m/z 269 $[M-H]^-$.

These two uncommon C16 oxylipins were first isolated from an axenic culture of the planktonic marine diatom *Thalassiosira rotula* [52] and characterized as their methyl ester derivatives. As to definitively confirm the structures of **5** and **6**, the mixture was treated with diazomethane, to obtain the corresponding methyl esters whose NMR and MS data were in agreement with literature. Oxylipins are a class of molecules produced from the oxidation of polyunsaturated fatty acids, by the action of lipoxygenase (LOX)/hydroperoxide lyase (HPL) enzymes. In diatoms, oxylipins are synthesized as grazing deterrence against copepods and sea urchins, after cell membranes breakage or cell senescence [17,53], but some investigations also indicated a key role in cell-to-cell signalling, regulation of the bacteria–phytoplankton community dynamics [54], and bloom events [55]. Currently, oxylipins are poorly studied for their biotechnological potential, however some reports demonstrated that oxylipins exerted anti-cancer activities, throught the activaction of apoptotic pathways, on different human cancer cell lines [56,57].

Finally, within the bioactive fractions derived from the butanolic soluble portion of *S. pinnata* only the chemical content of fraction B4 was investigated resulting in a mixture of purine nuclesosides with adenosine identified as main component by ^{1}H NMR analysis (Fig. 8.7).

3.3. Fatty acids profiling of the lipidic extract

The residual biomass, resulting from the first extraction step, was further subjected to a second extraction step using a solution of $CHCl_3$: CH_3OH (2:1 v/v) to obtain a lipidic extract, we characterized for its Fatty

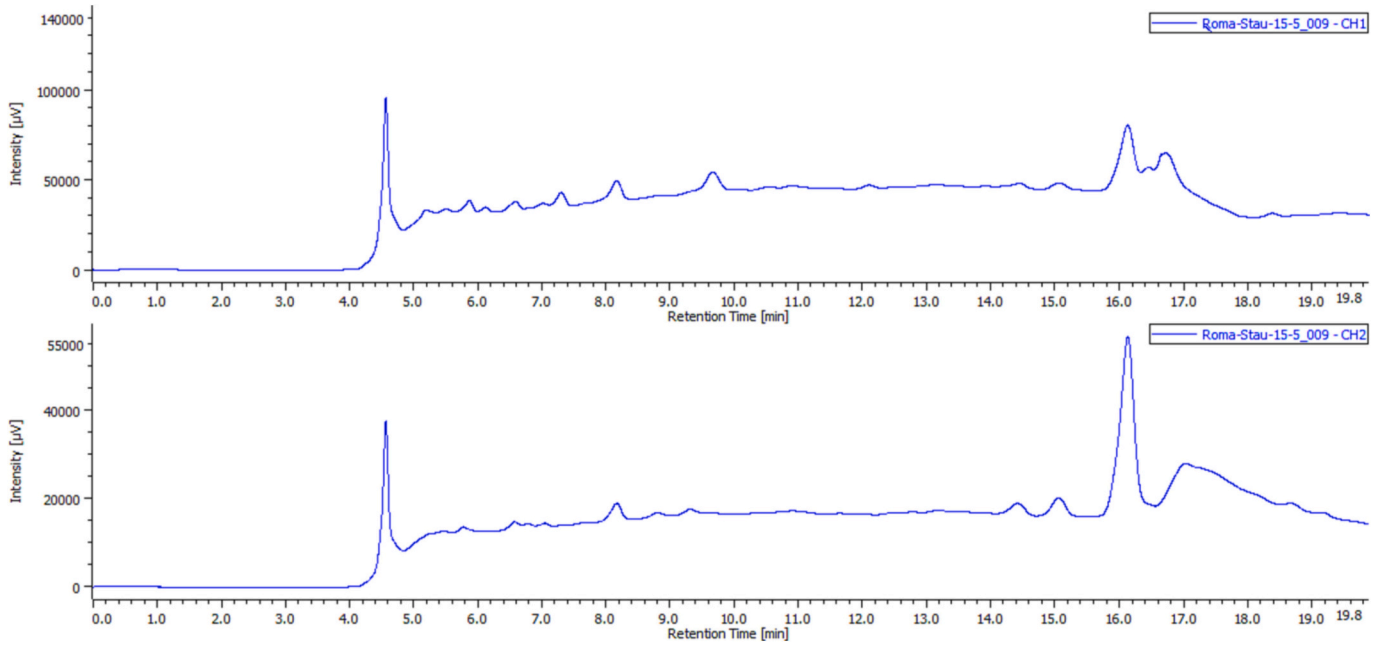

Fig. 6. HPLC profile of fraction A5.

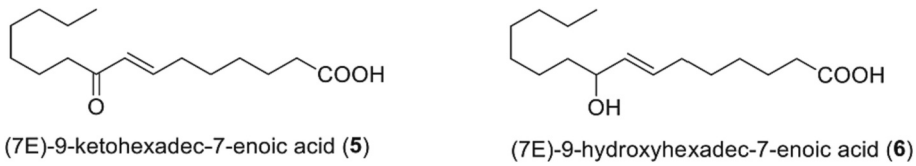

Fig. 7. Main components of fraction 5.

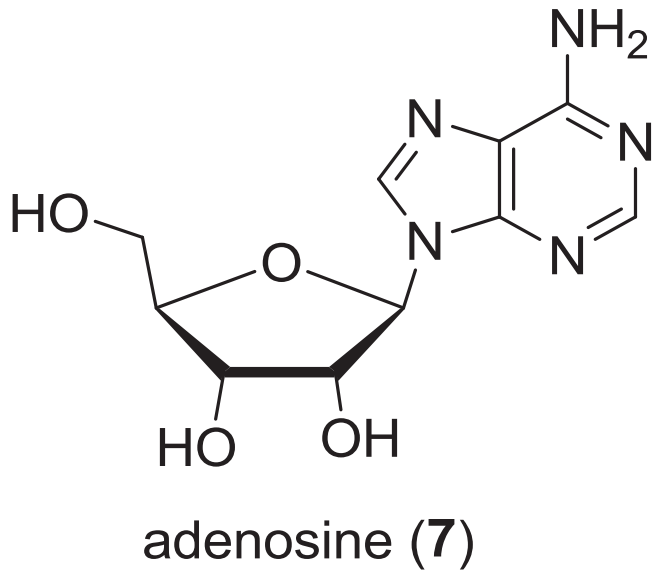

Fig. 8. Main component of the fraction B4.

Acids (FAs) composition.

GC-FID analysis (Fig. 9), showed that the main constituents of this lipidic extract are the hexadecanoic (C16:0, 31.02 %), the palmitoleic (C16:1, 25.95 %), and the eicosapentaenoic (EPA, C20:5, 10.58 %) acids, accounting for about 68 % of total Fas.Other FAs, such as the octadecanoic (C18:0), the myristic (C14:0), and the eicosatrienoic (C20:3n3) acids, were detected in a smaller percentage (6.51, 5.50, and 4.39 %, respectively).

These findings are in line with the ones previously reported for the same strain [32], with only small and neglectable differences in their relative abundance.

In addition, the lipidic extract profiling showed the abundance of FAs and ω3-Poly-Unsaturated Fatty Acids (PUFAs), with known biological activties on human cells. Indeed, ω3-PUFAs showed preventive and protective effects against cardiovascular diseases [58]; EPA administration counteracted insulin resistance and obesity [59], or suppressed oxidative stress, neuro-inflammation, and β-amyloid generation in the Alzheimer's disease, thus ameliorating the cognitive deficit associated to this pathology [60]; hexadecanoic acid was able to contrast proliferation in different cancer cell lines [61].

Our findings highlighted that *S. pinnata* could represent a promising source of bioactive lipids, exploitable for the nutraceutical and pharmaceutical fields.

3.4. Bioactivity of the lipidic extract on 3T3-L1 white adipose tissue cells

The administration of lipidic extract to the 3T3L-1 cell line resulted in a decrease of the lipid-droplet associated protein Perilipin 1 coupled to an increase of the phosphorylated form of the Hormone-Sensitive Lipase HSL660 (Fig. 10). This suggested that the lipidic extract was able to induce lipolysis which, through the generation of fatty acids, represents the primary energy source for mitochondria-sustained thermogenesis. In addition, no significant modulation of the mitochondrial Voltage Dependent Anion Channels 1 (VDAC1) was observed, indicating that the treatment did not affect mitochondrial mass. By contrast, the dose-dependent upregulation of the phosphorylated form of the

Fatty Acids	%
Butanoic acid (C4:0)	1.1155
Hexanoic acid (C6:0)	0.7672
Octanoic acid (C8:0)	0.8927
Decanoic acid (C10:0)	0.4038
Undecanoic acid (C11:0)	0.6267
Dodecanoic acid (C12:0)	0.7336
Tridecanoic acid (C13:0)	0.8333
Myristic acid (C14:0)	5.5043
Tetradecanoic acid (C14:1)	0.7716
Pentadecanoic acid (C15:0)	3.201
Pentadecenoic acid (C15:1)	1.2645
Hexadecanoic acid (C16:0)	31.0240
Palmitoleic acid (C16:1)	25.9528
Heptadecanoic acid (C17:1)	1.5953
Octadecanoic acid (C18:0)	6.5104
Oleic acid (C18:1 c+t)	0.6756
Linoleic acid (C18:2 c+t)	1.1863
(6Z,9Z,12Z)-Octadecatrienoic acid (C18:3n6)	1.9651
Eicosatrienoic acid (C20:3n3)	4.3959
Eicosapentaenoic acid (EPA) (C20:5)	10.5814

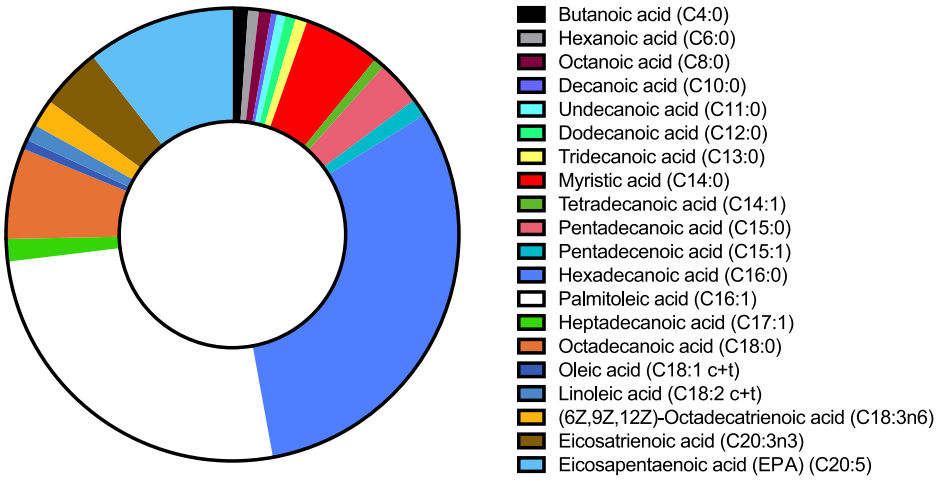

Fig. 9. Fatty acids composition of the lipid fraction extracted from *Staurosirella pinnata* residual biomass. Fatty Acids (FAs) profiles were qualitatively analyzed by means of GC-FID.

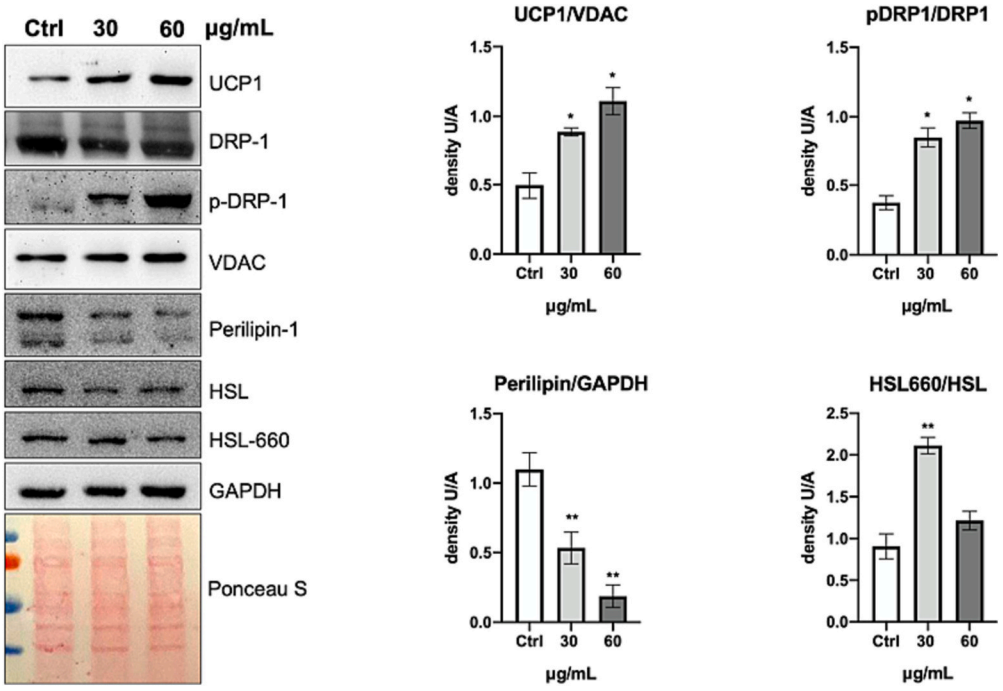

Fig. 10. Representative immunoblots and densitometry of UCP1/VDAC, pDRP-1/DRP-1, Perilipin/GAPDH and HSL660/HSL. Immunoblots are normalized using GAPDH. *, $p < 0.05$, **, $p < 0.01$, with respect to control cells. "Ctrl" refers to cells grown in DMEM supplied with the same solution (NaOH, BSA, and H2O) used to resuspend *S. pinnata* lipids.

Dynamin-Related Protein 1 (pDRP1) and of the Uncoupling Protein 1 (UCP1) suggested that the lipidic extract administration increased mitochondrial fission, a process crucial for enhancing UCP1 activity and the thermogenic potential of adipocyte mitochondria [62].

Metabolic activation of white adipose tissue (WAT), characterized by increased thermogenesis and lipolysis, is currently considered a promising pharmacological target to counteract obesity and type II diabetes mellitus [63]. The process, also called browning, depends upon the increased expression of key proteins, such as UCP1, thus making the white cell closer to a brown adipocyte, able to transform the stored fat into heat, thus improving glucose and lipids metabolism [64]. For this reason, in recent years, much effort has been made to identify compounds able to activate WAT metabolism. In this context, different reports highlighted that microalgal extracts can be considered as novel products with promising bioactivity against metabolic disorders. For example, the fucoxanthin-enriched extract of the diatom *Phaeodactylum*

tricornutum and the acqueous extract of *Euglena gracilis*, exhibited anti-obesity activities by regulating processes and metabolic pathways of therapeutic interest. Indeed, administration of *P. tricornutum* extract to the 3T3L-1 cell line, resulted in an increased expression of UCP1 and a down-regulation of the Peroxisome Proliferator-Activated Receptor gamma (PPARγ), a transcriptional factor that regulates fatty acid and glucose metabolisms in adipocytes [65], demonstrating the potential of this extract to reduce adipogenesis and blood glucose level; the administration of *E. gracilis* extract to hASCs cells (human adipose-derived stem cells) inhibited adipocyte-differentiation by the suppression of different regulators involved in that pathway, such as the fatty acid binding protein (AP2) and the lipoprotein lipase (LPL) [66], suggesting that this extract can be considered a promising candidate for the development of new therapeutic treatment against obesity.

Moreover, diet supplemented with microalgal biomass or with microalgal bioproducts (such as polysaccharides) proved to be able to reduce parameters involved in obesity, such as hyperglicemia, hypertriglyceridemia, dyslipidemia, body weight, and fat mass, in C57BL/6 mice and Wistar rats, highlighting the beneficial effects of the use of microalgae as food supplements for the treatment of metabolic syndromes even on *in vivo* models [67,68].

Our results clearly indicated the *S. pinnata* lipidic extract as a promising dietary supplement to counteract diabetes dysmetabolism and, thus, further investigations will be focused on the evaluation of its effects on *in vivo* models.

4. Conclusions

In this work *Staurosirella pinnata* biomass was biorefined to obtain several different co-products. Bioactivity tests on crude extract fractions showed that fraction A4 was particularly promising in terms of biomedical potential, being selectively cytotoxic when administered to the $BRAF^{V600E}$ human melanoma cell lines (A375), as compared to $BRAF^{wt}$ (CHL-1) and normal keratinocyte (HaCaT) cell lines. Different compounds, playing interesting roles *in vivo*, as chemical mediators, regulators, and in cell-to-cell signalling, have been identified and purified from this fraction: four apocarotenoids, previously described in the model organism *Phaeodactylum tricornutum*; two uncommon C16 oxylipins, first reported from *Thalassiosira rotula*; and the purine nucleoside adenosine.

Despite the presence of apocarotenoids is reported in plants, this is the first evidence on the production of apocarotenoids and oxylipins in the araphid, colonial diatom *S. pinnata* and, more in general, on apocarotenoids' production by mass cultivated microalgae. The biomedical potential of the second co-product, the lipidic extract, has also been demonstrated. This extract showed the modulation of molecular markers correlated to lipolysis and thermogenesis on white adipocytes (3T3-L1), presenting novel opportunities for the treatment of obesity and diabetes.

CRediT authorship contribution statement

Saverio Savio: Conceptualization, Data curation, Formal analysis, Investigation, Methodology, Validation, Visualization, Writing – original draft, Writing – review & editing. **Riccardo Turchi:** Data curation, Investigation, Validation. **Marianna Carbone:** Data curation, Formal analysis, Investigation, Methodology, Supervision, Validation, Visualization, Writing – original draft, Writing – review & editing. **Maria Letizia Ciavatta:** Data curation, Formal analysis, Investigation, Methodology, Validation, Visualization, Writing – original draft, Writing – review & editing. **Daniele Lettieri-Barbato:** Data curation, Validation, Visualization. **Katia Aquilano:** Conceptualization, Investigation, Methodology, Supervision, Validation, Visualization, Writing – original draft, Writing – review & editing. **Carlo Rodolfo:** Conceptualization, Data curation, Formal analysis, Investigation, Methodology, Supervision, Validation, Visualization, Writing – original draft, Writing – review & editing. **Roberta Congestri:** Conceptualization, Data curation, Formal analysis, Funding acquisition, Investigation, Methodology, Resources, Supervision, Validation, Visualization, Writing – original draft, Writing – review & editing.

Declaration of competing interest

The authors declare that they have no known competing financial interests or personal relationships that could have appeared to influence the work reported in this paper.

Data availability

Data will be made available on request.

Acknowledgements

M.C. and **M.L.C.** thank the European Commission – NextGenerationEU Projects "National Biodiversity Future Center", code n. N00000033, and "Strengthening the MIRRI Italian Research Infrastructure for Sustainable Bioscience and Bioeconomy, SUS MIRRI", code n. IR0000005.

S.S. and **R.C.** thank for the financial support the POR FESR Lazio 2014-2020, project 'AQUAFOOD'– "Microalgae for the removal of heavy metals and metalloids from water: safety of integrated food crops, recovery of algal products with high intrinsic/market value and recycling of water" funded by Regione Lazio.

S.S. thanks for the financial support the PhD program in Evolutionary Biology and Ecology of the University of Rome Tor Vergata.

References

[1] Lauritano Riccio, Microalgae with immunomodulatory activities, Mar. Drugs 18 (2019) 2, https://doi.org/10.3390/md18010002.
[2] T. Olasehinde, A. Olaniran, A. Okoh, Therapeutic potentials of microalgae in the treatment of Alzheimer's disease, Molecules 22 (2017) 480, https://doi.org/10.3390/molecules22030480.
[3] M.F.D.J. Raposo, A.M.M.B. de Morais, Microalgae for the prevention of cardiovascular disease and stroke, Life Sci. 125 (2015) 32–41, https://doi.org/10.1016/j.lfs.2014.09.018.
[4] K. Martínez Andrade, C. Lauritano, G. Romano, A. Ianora, Marine microalgae with anti-cancer properties, Mar. Drugs 16 (2018) 165, https://doi.org/10.3390/md16050165.
[5] C. Brownlee, K.E. Helliwell, Y. Meeda, D. McLachlan, E.A. Murphy, G.L. Wheeler, Regulation and integration of membrane transport in marine diatoms, Semin. Cell Dev. Biol. 134 (2023) 79–89, https://doi.org/10.1016/j.semcdb.2022.03.006.
[6] K.E. Helliwell, E.L. Harrison, J.A. Christie-Oleza, A.P. Rees, F.H. Kleiner, T. Gaikwad, J. Downe, M.M. Aguilo-Ferretjans, L. Al-Moosawi, C. Brownlee, G. L. Wheeler, A novel Ca2+ signaling pathway coordinates environmental phosphorus sensing and nitrogen metabolism in marine diatoms, Curr. Biol. 31 (2021) 978–989.e4, https://doi.org/10.1016/j.cub.2020.11.073.
[7] C.E. Hamm, R. Merkel, O. Springer, P. Jurkojc, C. Maier, K. Prechtel, V. Smetacek, Architecture and material properties of diatom shells provide effective mechanical protection, Nature 421 (2003) 841–843, https://doi.org/10.1038/nature01416.
[8] J.W. Herringer, D. Lester, G.E. Dorrington, G. Rosengarten, Can diatom girdle band pores act as a hydrodynamic viral defense mechanism? J. Biol. Phys. 45 (2019) 213–234, https://doi.org/10.1007/s10867-019-09525-5.
[9] M. Ellegaard, T. Lenau, N. Lundholm, C. Maibohm, S.M.M. Friis, K. Rottwitt, Y. Su, The fascinating diatom frustule—can it play a role for attenuation of UV radiation? J. Appl. Phycol. 28 (2016) 3295–3306, https://doi.org/10.1007/s10811-016-0893-5.
[10] L.E. Aguirre, L. Ouyang, A. Elfwing, M. Hedblom, A. Wulff, O. Inganäs, Diatom frustules protect DNA from ultraviolet light, Sci. Rep. 8 (2018) 5138, https://doi.org/10.1038/s41598-018-21810-2.
[11] G.J. Doucette, K.L. King, A.E. Thessen, Q. Dortch, The effect of salinity on domoic acid production by the diatom *Pseudo-nitzschia multiseries*, Nova Hedwigia 133 (2008) 31–46.
[12] N. Lundholm, B. Krock, U. John, J. Skov, J. Cheng, M. Pančić, S. Wohlrab, K. Rigby, T.G. Nielsen, E. Selander, S. Harðardóttir, Induction of domoic acid production in diatoms—types of grazers and diatoms are important, Harmful Algae 79 (2018) 64–73, https://doi.org/10.1016/j.hal.2018.06.005.
[13] M.P. Sison-Mangus, S. Jiang, R.M. Kudela, S. Mehic, Phytoplankton-associated bacterial community composition and succession during toxic diatom bloom and non-bloom events, Front. Microbiol. 7 (2016) 1433, https://doi.org/10.3389/fmicb.2016.01433.

[14] N. Ruocco, L. Albarano, R. Esposito, V. Zupo, M. Costantini, A. Ianora, Multiple roles of diatom-derived oxylipins within marine environments and their potential biotechnological applications, Mar. Drugs 18 (2020) 342, https://doi.org/10.3390/md18070342.
[15] E. Gudimova, H.C. Eilertsen, T.Ø. Jørgensen, E. Hansen, In vivo exposure to northern diatoms arrests sea urchin embryonic development, Toxicon 109 (2016) 63–69, https://doi.org/10.1016/j.toxicon.2015.11.001.
[16] N. Ruocco, C. Annunziata, A. Ianora, G. Libralato, L. Manfra, S. Costantini, M. Costantini, Toxicity of diatom-derived polyunsaturated aldehyde mixtures on sea urchin *Paracentrotus lividus* development, Sci. Rep. 9 (2019) 517, https://doi.org/10.1038/s41598-018-37546-y.
[17] G. Pohnert, Diatom/copepod interactions in plankton: the indirect chemical defense of unicellular algae, ChemBioChem 6 (2005) 946–959, https://doi.org/10.1002/cbic.200400348.
[18] J. Frenkel, C. Wess, W. Vyverman, G. Pohnert, Chiral separation of a diketopiperazine pheromone from marine diatoms using supercritical fluid chromatography, J. Chromatogr. B 951–952 (2014) 58–61, https://doi.org/10.1016/j.jchromb.2013.12.040.
[19] F. Klapper, S. Audoor, W. Vyverman, G. Pohnert, Pheromone mediated sexual reproduction of pennate diatom *Cylindrotheca closterium*, J. Chem. Ecol. 47 (2021) 504–512, https://doi.org/10.1007/s10886-021-01277-8.
[20] J. Gillard, J. Frenkel, V. Devos, K. Sabbe, C. Paul, M. Rempt, D. Inzé, G. Pohnert, M. Vuylsteke, W. Vyverman, Metabolomics enables the structure elucidation of a diatom sex pheromone, Angew. Chem. Int. Ed. 52 (2013) 854–857, https://doi.org/10.1002/anie.201208175.
[21] C.M. Osuna-Cruz, G. Bilcke, E. Vancaester, S. De Decker, A.M. Bones, P. Winge, N. Poulsen, P. Bulankova, B. Verhelst, S. Audoor, D. Belisova, A. Pargana, M. Russo, F. Stock, E. Cirri, T. Brembu, G. Pohnert, G. Piganeau, M.I. Ferrante, T. Mock, L. Sterck, K. Sabbe, L. De Veylder, W. Vyverman, K. Vandepoele, The *Seminavis robusta* genome provides insights into the evolutionary adaptations of benthic diatoms, Nat. Commun. 11 (2020) 3320, https://doi.org/10.1038/s41467-020-17191-8.
[22] K.-N. Kim, S.-J. Heo, W.-J. Yoon, S.-M. Kang, G. Ahn, T.-H. Yi, Y.-J. Jeon, Fucoxanthin inhibits the inflammatory response by suppressing the activation of NF-κB and MAPKs in lipopolysaccharide-induced RAW 264.7 macrophages, Eur. J. Pharmacol. 649 (2010) 369–375, https://doi.org/10.1016/j.ejphar.2010.09.032.
[23] H.A. Hussein, M.A. Abdullah, Anticancer compounds derived from marine diatoms, Mar. Drugs 18 (2020) 356, https://doi.org/10.3390/md18070356.
[24] J. Pekkoh, K. Phinyo, T. Thurakit, S. Lomakool, K. Duangjan, K. Ruangrit, C. Pumas, S. Jiranusornkul, W. Yooin, B. Cheirsilp, W. Pathom-aree, S. Srinuanpan, Lipid profile, antioxidant and antihypertensive activity, and computational molecular docking of diatom fatty acids as ACE inhibitors, Antioxidants 11 (2022) 186, https://doi.org/10.3390/antiox11020186.
[25] D.F. Ramos, P.C. Bartolomeu Halicki, C. da Silva Canielles, P. Caprara, C. da R. M. D'Oca Borges, M. de Fátima, C. Santos, M.G.M. D'Oca, F. Roselet, P.E. Almeida da Silva, P.C. Abreu, Chemical profile and antimicrobial activity of the marine diatom *Chaetoceros muelleri*, Chem. Biodivers. 19 (2022) e202100846, https://doi.org/10.1002/cbdv.202100846.
[26] C. Sansone, P. Concetta, G. Christian, S. Arianna, B. Antonino, N. Douglas, A. Adriana, B. Christophe, Abstract 25: *Skeletonema marinoi* (diatom) extracts are endowed with promising cancer preventive properties in prostate cancer cells, Cancer Res. 80 (2020) 25, https://doi.org/10.1158/1538-7445.AM2020-25.
[27] S. Savio, R. Congestri, C. Rodolfo, Are we out of the infancy of microalgae-based drug discovery? Algal Res. 54 (2021) 102173 https://doi.org/10.1016/j.algal.2020.102173.
[28] L.A. Martín, C.A. Popovich, A.M. Martínez, P.G. Scodelaro Bilbao, M.C. Damiani, P. I. Leonardi, Hybrid two-stage culture of *Halamphora coffeaeformis* for biodiesel production: growth phases, nutritional stages and biorefinery approach, Renew. Energy 118 (2018) 984–992, https://doi.org/10.1016/j.renene.2017.10.086.
[29] Y. Cui, S.R. Thomas-Hall, E.T. Chua, P.M. Schenk, Development of a *Phaeodactylum tricornutum* biorefinery to sustainably produce omega-3 fatty acids and protein, J. Clean. Prod. 300 (2021) 126839, https://doi.org/10.1016/j.jclepro.2021.126839.
[30] M. Francavilla, P. Kamaterou, S. Intini, M. Monteleone, A. Zabaniotou, Cascading microalgae biorefinery: fast pyrolysis of *Dunaliella tertiolecta* lipid extracted-residue, Algal Res. 11 (2015) 184–193, https://doi.org/10.1016/j.algal.2015.06.017.
[31] J. Monte, C. Ribeiro, C. Parreira, L. Costa, L. Brive, S. Casal, C. Brazinha, J. G. Crespo, Biorefinery of *Dunaliella salina*: sustainable recovery of carotenoids, polar lipids and glycerol, Bioresour. Technol. 297 (2020) 122509, https://doi.org/10.1016/j.biortech.2019.122509.
[32] S. Savio, S. Farrotti, D. Paris, E. Arnaìz, I. Díaz, S. Bolado, R. Muñoz, C. Rodolfo, R. Congestri, Value-added co-products from biomass of the diatoms *Staurosirella pinnata* and *Phaeodactylum tricornutum*, Algal Res. 47 (2020) 101830, https://doi.org/10.1016/j.algal.2020.101830.
[33] S. Savio, S. Farrotti, A. Di Giulio, S. De Santis, N.T.W. Ellwood, S. Ceschin, R. Congestri, Functionalization of frustules of the diatom *Staurosirella pinnata* for nickel (Ni) adsorption from contaminated aqueous solutions, Front. Mar. Sci. 9 (2022) 581, https://doi.org/10.3389/fmars.2022.889832.
[34] E.G. Bligh, W.J. Dyer, A rapid method of total lipid extraction and purification, Can. J. Biochem. Physiol. 37 (1959) 911–917, https://doi.org/10.1139/o59-099.
[35] C. Rodolfo, M. Rocco, L. Cattaneo, M. Tartaglia, M. Sassi, P. Aducci, A. Scaloni, L. Camoni, M. Marra, Ophiobolin a induces autophagy and activates the mitochondrial pathway of apoptosis in human melanoma cells, PLoS One 11 (2016) e0167672, https://doi.org/10.1371/journal.pone.0167672.
[36] P. Chakrabarti, K.V. Kandror, FoxO1 controls insulin-dependent adipose triglyceride lipase (ATGL) expression and lipolysis in adipocytes, J. Biol. Chem. 284 (2009) 13296–13300, https://doi.org/10.1074/jbc.C800241200.
[37] E.R. Cantwell-Dorris, J.J. O'Leary, O.M. Sheils, BRAFV600E: implications for carcinogenesis and molecular therapy, Mol. Cancer Ther. 10 (2011) 385–394, https://doi.org/10.1158/1535-7163.MCT-10-0799.
[38] G. Riccio, K.A. Martinez, A. Ianora, C. Lauritano, De novo transcriptome of the flagellate *Isochrysis galbana* identifies genes involved in the metabolism of antiproliferative metabolites, Biology (Basel) 11 (2022) 771, https://doi.org/10.3390/biology11050771.
[39] R. Ciarcia, C. Longobardi, G. Ferrara, S. Montagnaro, E. Andretta, F. Pagnini, S. Florio, L. Maruccio, C. Lauritano, S. Damiano, The microalga *Skeletonema marinoi* induces apoptosis and DNA damage in K562 cell line by modulating NADPH oxidase, Molecules 27 (2022) 8270, https://doi.org/10.3390/molecules27238270.
[40] G. Nuzzo, B. Gomes, C. Gallo, P. Amodeo, C. Sansone, O. Pessoa, E. Manzo, R. Vitale, A. Ianora, E. Santos, L. Costa-Lotufo, A. Fontana, Potent cytotoxic analogs of Amphidinolides from the Atlantic octocoral *Stragulum bicolor*, Mar. Drugs 17 (2019) 58, https://doi.org/10.3390/md17010058.
[41] J. Kimura, N. Maki, New Loliolide derivatives from the brown alga *Undaria pinnatifida*, J. Nat. Prod. 65 (2002) 57–58, https://doi.org/10.1021/np0103057.
[42] A. Felemban, J. Braguy, M.D. Zurbriggen, S. Al-Babili, Apocarotenoids involved in plant development and stress response, Front. Plant Sci. 10 (2019) 478231, https://doi.org/10.3389/fpls.2019.01168.
[43] J.Y. Wang, P.-Y. Lin, S. Al-Babili, On the biosynthesis and evolution of apocarotenoid plant growth regulators, Semin. Cell Dev. Biol. 109 (2021) 3–11, https://doi.org/10.1016/j.semcdb.2020.07.007.
[44] J.C. Moreno, J. Mi, Y. Alagoz, S. Al-Babili, Plant apocarotenoids: from retrograde signaling to interspecific communication, Plant J. 105 (2021) 351–375, https://doi.org/10.1111/tpj.15102.
[45] M. Zoccali, D. Giuffrida, F. Salafia, C. Socaciu, K. Skjånes, P. Dugo, L. Mondello, First apocarotenoids profiling of four microalgae strains, Antioxidants 8 (2019) 209, https://doi.org/10.3390/antiox8070209.
[46] B.A. Shaw, R.J. Andersen, P.J. Harrison, Feeding deterrence properties of apo-fucoxanthinoids from marine diatoms. I. Chemical structures of apo-fucoxanthinoids produced by Phaeodactylum tricornutum, Mar. Biol. 124 (1995) 467–472, https://doi.org/10.1007/BF00363921.
[47] M.H. Walter, D. Strack, Carotenoids and their cleavage products: biosynthesis and functions, Nat. Prod. Rep. 28 (2011) 663, https://doi.org/10.1039/c0np00036a.
[48] K.N. Gangadhar, M.J. Rodrigues, H. Pereira, H. Gaspar, F.X. Malcata, L. Barreira, J. Varela, Anti-hepatocellular carcinoma (HepG2) activities of monoterpene hydroxy lactones isolated from the marine microalga *Tisochrysis lutea*, Mar. Drugs 18 (2020) 567, https://doi.org/10.3390/md18110567.
[49] S. Komba, E. Kotake-Nara, W. Tsuzuki, Degradation of fucoxanthin to elucidate the relationship between the fucoxanthin molecular structure and its antiproliferative effect on Caco-2 cells, Mar. Drugs 16 (2018) 275, https://doi.org/10.3390/md16080275.
[50] S.I. Bukhari, M. Manzoor, M.K. Dhar, A comprehensive review of the pharmacological potential of *Crocus sativus* and its bioactive apocarotenoids, Biomed. Pharmacother. 98 (2018) 733–745, https://doi.org/10.1016/j.biopha.2017.12.090.
[51] C. Zhang, Biosynthesis of carotenoids and apocarotenoids by microorganisms and their industrial potential, in: Prog, Carotenoid Res, InTech, 2018, https://doi.org/10.5772/intechopen.79061.
[52] G. d'Ippolito, A. Cutignano, R. Briante, F. Febbraio, G. Cimino, A. Fontana, New C16 fatty-acid-based oxylipin pathway in the marine diatom *Thalassiosira rotula*, Org. Biomol. Chem. 3 (2005) 4065, https://doi.org/10.1039/b510640k.
[53] R. Esposito, N. Ruocco, L. Albarano, A. Ianora, L. Manfra, G. Libralato, M. Costantini, Combined effects of diatom-derived oxylipins on the sea urchin *Paracentrotus lividus*, Int. J. Mol. Sci. 21 (2020) 719, https://doi.org/10.3390/ijms21030719.
[54] E.R. Brown, M.R. Cepeda, S.J. Mascuch, K.L. Poulson-Ellestad, J. Kubanek, Chemical ecology of the marine plankton, Nat. Prod. Rep. 36 (2019) 1093–1116, https://doi.org/10.1039/C8NP00085A.
[55] C. Vidoudez, G. Pohnert, Growth phase-specific release of polyunsaturated aldehydes by the diatom *Skeletonema marinoi*, J. Plankton Res. 30 (2008) 1305–1313, https://doi.org/10.1093/plankt/fbn085.
[56] C. Sansone, A. Braca, E. Ercolesi, G. Romano, A. Palumbo, R. Casotti, M. Francone, A. Ianora, Diatom-derived polyunsaturated aldehydes activate cell death in human cancer cell lines but not normal cells, PLoS One 9 (2014) e101220, https://doi.org/10.1371/journal.pone.0101220.
[57] M.L. Edin, C. Duval, G. Zhang, D.C. Zeldin, Role of linoleic acid-derived oxylipins in cancer, Cancer Metastasis Rev. 39 (2020) 581–582, https://doi.org/10.1007/s10555-020-09904-8.
[58] T.D. O'Connell, R.P. Mason, M.J. Budoff, A.M. Navar, G.C. Shearer, Mechanistic insights into cardiovascular protection for omega-3 fatty acids and their bioactive lipid metabolites, Eur. Hear. J. Suppl. 22 (2020) J3–J20, https://doi.org/10.1093/eurheartj/suaa115.
[59] E.J. Baker, E.A. Miles, G.C. Burdge, P. Yaqoob, P.C. Calder, Metabolism and functional effects of plant-derived omega-3 fatty acids in humans, Prog. Lipid Res. 64 (2016) 30–56, https://doi.org/10.1016/j.plipres.2016.07.002.
[60] H. Che, M. Zhou, T. Zhang, L. Zhang, L. Ding, T. Yanagita, J. Xu, C. Xue, Y. Wang, EPA enriched ethanolamine plasmalogens significantly improve cognition of Alzheimer's disease mouse model by suppressing β-amyloid generation, J. Funct. Foods 41 (2018) 9–18, https://doi.org/10.1016/j.jff.2017.12.016.

[61] H. Harada, U. Yamashita, H. Kurihara, E. Fukushi, J. Kawabata, Y. Kamei, Antitumor activity of palmitic acid found as a selective cytotoxic substance in a marine red alga, Anticancer Res. 22 (2002) 2587–2590. http://www.ncbi.nlm.nih.gov/pubmed/12529968.

[62] D.F. Pisani, V. Barquissau, J.-C. Chambard, D. Beuzelin, R.A. Ghandour, M. Giroud, A. Mairal, S. Pagnotta, S. Cinti, D. Langin, E.-Z. Amri, Mitochondrial fission is associated with UCP1 activity in human brite/beige adipocytes, Mol. Metab. 7 (2018) 35–44, https://doi.org/10.1016/j.molmet.2017.11.007.

[63] A. Pfeifer, L.S. Hoffmann, Brown, beige, and white: the new color code of fat and its pharmacological implications, Annu. Rev. Pharmacol. Toxicol. 55 (2015) 207–227, https://doi.org/10.1146/annurev-pharmtox-010814-124346.

[64] M. di Somma, M. Vliora, E. Grillo, B. Castro, E. Dakou, W. Schaafsma, J. Vanparijs, M. Corsini, C. Ravelli, E. Sakellariou, S. Mitola, Role of VEGFs in metabolic disorders, Angiogenesis 23 (2020) 119–130, https://doi.org/10.1007/s10456-019-09700-1.

[65] S.Y. Koo, J.-H. Hwang, S.-H. Yang, J.-I. Um, K.W. Hong, K. Kang, C.-H. Pan, K. T. Hwang, S.M. Kim, Anti-obesity effect of standardized extract of microalga *Phaeodactylum tricornutum* containing fucoxanthin, Mar. Drugs 17 (2019) 311, https://doi.org/10.3390/md17050311.

[66] R. Sugimoto, N. Ishibashi-Ohgo, K. Atsuji, Y. Miwa, O. Iwata, A. Nakashima, K. Suzuki, *Euglena* extract suppresses adipocyte-differentiation in human adipose-derived stem cells, PLoS One 13 (2018) e0192404, https://doi.org/10.1371/journal.pone.0192404.

[67] C. Mayer, L. Richard, M. Côme, L. Ulmann, H. Nazih, B. Chénais, K. Ouguerram, V. Mimouni, The marine microalga, *Tisochrysis lutea*, protects against metabolic disorders associated with metabolic syndrome and obesity, Nutrients 13 (2021) 430, https://doi.org/10.3390/nu13020430.

[68] W. Guo, S. Zhu, S. Li, Y. Feng, H. Wu, M. Zeng, Microalgae polysaccharides ameliorates obesity in association with modulation of lipid metabolism and gut microbiota in high-fat-diet fed C57BL/6 mice, Int. J. Biol. Macromol. 182 (2021) 1371–1383, https://doi.org/10.1016/j.ijbiomac.2021.05.067.